JOURNAL OF COMPUTATIONAL PHYSICS 61, 119–137 (1985)

A General, Non-Iterative Riemann Solver for Godunov's Method*

JOHN K. DUKOWICZ

Theoretical Division, Group T-3, University of California, Los Alamos National Laboratory, Los Alamos, New Mexico 87545

Received June 28, 1984

Godunov's method is characterized by the use of a Riemann problem solution to resolve discontinuities at the interface between cells. The major drawback of this method is the difficulty and the high cost of solving the (nonlinear) Riemann problem exactly, especially for materials with complex equations of state. This paper describes a simplified and noniterative approximate Riemann solver which is characterized by only two material-dependent parameters. For a given material, these parameters are the local speed of sound and a parameter which is directly related to the shock density ratio in the limit of strong shocks. These parameters are conveniently obtained from a linear fit to the experimental data for the shock Hugoniot in various materials. The approximate Riemann solver retains the essential quadratic nonlinearity which enables it to deal with the whole range of cases from weak sound waves to strong shocks.

I. INTRODUCTION

The introduction of the concept of artificial shock viscosity by von Neumann and Richtmyer [1] in 1950 permitted for the first time the development of practical numerical methods for problems involving strong shock waves. The basic idea was to spread the thickness of a shock wave over several computational cells, allowing the numerical method to resolve, and therefore "capture" the shock wave. The great utility and simplicity of the method accounts for its widespread and continuing popularity. The main drawback of the method is that in practical usage it frequently produces either overly thick, or oscillatory, shock profiles since there is some uncertainty about the appropriate values of coefficients to be used under varying conditions and for different equations of state.

In 1959 a radically different, alternative method was published by Godunov [2]. He proposed to consider all quantities in a computational cell to be constant at the start of a time step, given by the cell mass-weighted average, and to resolve the

* The U.S. Government's right to retain a nonexclusive royalty-free license in and to the copyright covering this paper, for governmental purposes, is acknowledged. The Los Alamos National Laboratory is operated by the University of California for the United States Department of Energy under contract W-7405-ENG-36.

0021-9991/85 $3.00

581/61/1-9

resultant discontinuities at the cell edges by the solution of a Riemann problem. The great advantage of this method is the clear physical picture of the interactions involved, and the absence of any arbitrary parameters. The method naturally and automatically handles shock waves, interfaces between different materials, free surfaces, and predicts cavitation should it occur. In practice the method is characterized by nearly optimally thin shocks, typically one to three cells wide [3]. From the mathematical point of view it has the desirable properties of monotonicity [2], and the physically correct flow of information [4]. The main drawback of the method, which has limited its widespread usage, is the difficulty and the high cost of solving the (nonlinear) Riemann problem exactly, especially for materials with complex equations of state, which are frequently available only in tabular form. This has led to various attempts to approximate the Riemann problem. One of the first approximations, by Godunov *et al.* [5], was to replace all waves in the Riemann problem by sound waves, in cases when the waves were expected to be weak. This amounted to, in effect, the use of only one iteration in the solution of the Riemann problem.

The use of Godunov's method has recently attracted new interest in the field of aerodynamics. Here one expects to encounter only ideal gas (polytropic) equations of state. This simplification has permitted the development of several successful linear approximations, among them the methods due to Enquist and Osher [6]. Roe [7], and Pandolfi [8].

Another direction in the development of Godunov's method was taken by van Leer [9]. He proposed to represent the distribution of variables in a cell by piecewise linear segments, limited in such a way as to preserve monotonicity. The remaining discontinuities at the cell edges were again to be resolved by the solution of a Riemann problem. This modification improved the formal accuracy of Godunov's method to second order in the smooth regions of the flow. Further developments along this line, also in the context of the ideal gas equation of state, are represented by the work of Colella and Woodward [10, 11].

Since both the method of artificial shock viscosity and Godunov's method are general shock capturing methods, it is not a coincidence that there is a close relationship between them. One can view the effect of either method to be the introduction of an appropriate amount of entropy into the flow. In the artificial viscosity method the entropy is added by the dissipation produced by the artificial viscosity, while in Godunov's method the entropy increase is (principally) produced implicitly by the presence of shock waves resulting from the Riemann problem. In fact, it has been noticed that the shock Hugoniot curve (the shock pressure jump as a function of the velocity jump), in those cases when it can be found explicitly, closely resembles the form of the artificial shock viscosity commonly used [12]. This close relationship is exploited in this paper to derive an approximation to the solution of the Riemann problem that is both noniterative and remarkably accurate. Just as the method of artificial shock viscosity is found to be effective for arbitrary materials, the new method is equally general, but in addition, it retains all the advantages of the exact Godunov method.

II. Preliminaries

A. *Conservation Equations*

We are interested in the (Euler) equations of multidimensional, inviscid, compressible fluid dynamics. The solution of these equations can always be divided into a Lagrangian phase, followed by a rezone or remap phase. In the Lagrangian phase the computational cell boundaries are assumed to move with the local flow velocity. The rezone or remap phase is an interpolation procedure that transfers quantities from one computational mesh to another, generally in a conservative manner, at any time in the computation that such a transfer is desired [13]. This phase is completely independent of the Lagrangian phase, and in the present context is of little interest since it is only coordinate-system dependent, and in this sense has no fluid dynamics content. For simplicity, therefore, we shall restrict our attention to the Lagrangian phase.

Conservative computational methods are generally based on the control volume formulation of the conservation equations [14]. The Lagrangian form of the control volume equations may be written as

$$m_k \frac{d\bar{\mathbf{u}}_k}{dt} = -\int_{S_k} p\mathbf{n}dA. \tag{1}$$

$$m_k \frac{d\bar{E}_k}{dt} = -\int_{S_k} p\mathbf{u}\cdot\mathbf{n}dA, \tag{2}$$

where $m_k = \int_{V_k} \rho dV$ is the cell mass, $\bar{\mathbf{u}}_k = (1/m_k)\int_{V_k} \rho \mathbf{u} dV$ is the cell averaged velocity, $\bar{E}_k = (1/m_k)\int_{V_k} \rho(e + \frac{1}{2}\mathbf{u}\cdot\mathbf{u})\, dV$ is the average total energy, ρ is the density, e is the specific internal energy and $\mathbf{u}$ is the local velocity. The control volume is taken to be the computational cell with volume V_k and surface S_k, with outward unit vector $\mathbf{n}$ normal to the surface. The pressure p is given by the equation of state $p = p(\rho, e)$. We note that to advance the solution of Eqs. (1) and (2) in time we need only the pressure and velocity at cell boundaries. Conservation of mass is expressed by $dm_k/dt = 0$, and the kinematics of the cell motion are given by $d\mathbf{x}/dt = \mathbf{u}$.

B. *The Artificial Shock Viscosity Method* [3, 12]

The artificial shock viscosity method is commonly implemented using the "staggered" control volume formulation, and also frequently (but not necessarily) using an internal energy equation rather than Eq. (2) [3]. In using the staggered mesh one introduces additional control volumes associated with the momentum equation, located either around cell faces or cell vertices, depending on where the velocities are assumed to be located.

Considering the 1-dimensional case for simplicity, the cell pressure p is augmented by an artificial shock viscosity contribution q as follows:

$$p' = p + q,$$

and it is this augmented p' that is used in the momentum and energy equations. The original von Neumann ("quadratic") form of q is

$$q_1 = c_0^2 \rho (\Delta x)^2 \left(\frac{\partial u}{\partial x}\right)^2,$$
$$= c_0^2 \rho \Delta u^2, \tag{3}$$

where Δx is the cell dimension, Δu is the velocity difference across the cell, and c_0 is a constant (≈ 2). In 1955 Landshoff [15] introduced another ("linear") form of q,

$$q_2 = c_L \rho a_0 \Delta x \left|\frac{\partial u}{\partial x}\right|,$$
$$= c_L \rho a_0 |\Delta u|, \tag{4}$$

where a_0 is the local speed of sound, and c_L is a constant (≈ 1). The recommended [12, 15] form of q is a combination of the two:

$$q = q_1 + q_2,$$
$$= c_0^2 \rho \Delta u^2 + c_L \rho a_0 |\Delta u| \tag{5}$$

Typically q is set to zero when $\Delta u \geqslant 0$, that is, when the flow is expanding. Although q is treated as a pressure it is usually interpreted as a form of bulk viscosity. It is remarkable that this method is apparently capable of handling all situations with an appropriate adjustment of the coefficients c_0, c_L. However, there is some uncertainty in specifying the correct values of these parameters, and in multidimensions, in specifying the appropriate cell length Δx.

C. *The Godunov Method* [1, 3]

The original Godunov method solves equations directly in the form of Eqs. (1) and (2). The cell averaged quantities $\bar{\mathbf{u}}_k$, $\bar{E}_k$, and $\bar{\rho}_k = m_k/V_k$ are used to obtain initial data for a Riemann problem at each cell interface. These data, on either side of the interface, are

(a) $w_k = \mathbf{n} \cdot \bar{\mathbf{u}}_k$, the normal velocity,

(b) $\bar{e}_k = \bar{E}_k - \frac{1}{2}\bar{\mathbf{u}}_k \cdot \bar{\mathbf{u}}_k$, the specific internal energy,

(c) $\bar{\rho}_k$, the density, and

(d) $\bar{p}_k = p(\bar{\rho}_k, \bar{e}_k)$, the equation of state pressure.

The Riemann problem is illustrated in Fig. 1 in terms of an x–t diagram. The data of the initial discontinuity are specified by ρ_L, e_L, p_L, w_L on the left side, and ρ_R, e_R, p_R, and w_R on the right side of the discontinuity. Velocities are assumed to be positive towards the right. The initial discontinuity is resolved by a system of waves which consists of a contact discontinuity and a wave on either side, which may be

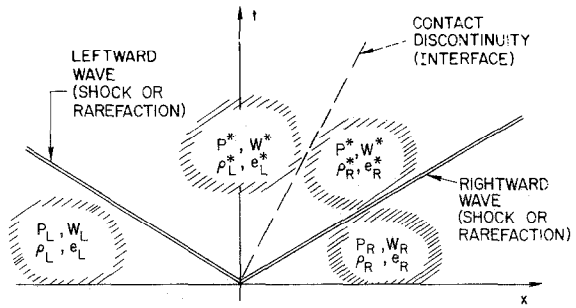

FIG. 1. A schematic representation of the wave system in a general Riemann problem.

either a shock wave or a rarefaction fan. In the absence of cavitation the pressure and velocity on either side of the contact discontinuity are equal and are given by p^* and w^*, while the density and internal energy are discontinuous and are denoted by ρ_L^*, e_L^* on the left of the interface, and ρ_R^*, e_R^* on the right.

The Riemann problem, and its solution in terms of p-w curves is discussed by Courant and Friedrichs [16]. The solution provides the values of the pressure p^* and the normal velocity w^* of the contact discontinuity. The contact discontinuity represents the cell interface following the resolution of the initial discontinuity by the wave system of the Riemann problem, and so these are exactly the quantities needed on the right hand side of Eqs. (1) and (2) to advance the solution in time. The interface pressure p^* and velocity w^* are unique except in the case of cavitation when two interfaces are established, each with its own velocity. We will proceed now to describe the Riemann problem and its approximation. Other details of the Godunov method (or its higher accuracy developments) will be omitted and may be found in the literature.

Let us consider shock waves first, and introduce the specific volume $v \equiv 1/\rho$ to simplify the formulation. The Rankine–Hugoniot relations give

$$\Delta w_S = \pm [-\Delta p_S / \Delta v_S]^{1/2} \Delta v_S, \tag{6}$$

$$\Delta e_S = -\tfrac{1}{2} [p_S + p^*] \Delta v_S, \tag{7}$$

where $\Delta w_S = w^* - w_S$, $\Delta v_S = v_S^* - v_S$, etc., and the subscript S represents L or R, for leftward- or rightward-going waves. In Eq. (6) the upper sign corresponds to leftward-, and the lower sign to rightward-going waves. With the equation of state specified as $p = p(e, v)$, the above two equations implicitly define the Hugoniot curve

$$\Delta p_S = \mp |W_S| \Delta w_S, \tag{8}$$

where $|W_S|$ is a positive function of Δp_S, or alternatively, of Δw_S alone.

Similarly, for rarefaction waves we can write the corresponding simultaneous differential equations

$$\frac{dw}{dv} = \pm\left[-\frac{dp}{dv}\right]^{1/2},$$

$$\frac{de}{dv} = -p,$$

where $dp/dv = \partial p/\partial v + (\partial p/\partial e)(de/dv)$ from the equation of state. These two equations may be simultaneously integrated to give

$$\Delta w_S = \pm \int_{v_S}^{v_S^*} \left[-\frac{dp}{dv}\right]^{1/2} dv, \tag{9}$$

$$\Delta e_S = -\int_{v_S}^{v_S^*} p\, dv, \tag{10}$$

corresponding to Eqs. (6) and (7). Similarly, these equations imply

$$\Delta p_S = \mp |V_S|\, \Delta w_S, \tag{11}$$

where $|V_S|$ is the corresponding positive function associated with transition through a rarefaction wave. The choice between Eqs. (8) and (11) is made according to whether p^* is greater than or less than p_S.

There are four cases to consider. Let us assume that we expect the rightward wave to be a shock, and the leftward wave to be a rarefaction. For this case we have

$$p^* - p_L = -|V_L|\, \Delta w_L,$$

$$p^* - p_R = |W_R|\, \Delta w_R.$$

Subtracting to eliminate p^* we obtain

$$|W_R|\, \Delta w_R + |V_L|\, \Delta w_L + p_R - p_L = 0, \tag{12}$$

an implicit equation in w^* provided $|W_R|$ and $|V_L|$ are expressed in terms of velocity differences. The solution must be consistent with the initial assumption that $p^* \leqslant p_L$ and $p^* \geqslant p_R$, or else another case must be considered.

Explicit expressions for $|V_S|$ and $|W_S|$ are available only in special cases, such as the ideal gas equation of state. For this case, Eq. (12) (or the corresponding equation in p^*) can be efficiently solved using a Newton–Raphson method [9]. In the general case, a single equation such as (12) cannot be obtained and so the iterative solution is more difficult. Further difficulties are encountered when the equation of state is available in tabular form only, or when equation of state

evaluations are expensive. An approximate but still iterative method has been proposed by Colella and Glaz [17] to overcome some of these difficulties.

We now turn to a description of the new simplified method. Two separate approximations are involved.

III. The Approximate Riemann Problem

A. *The Two-Shock Approximation*

Comparing Eqs. (6) and (7) to Eqs. (9) and (10) we notice that the shock equations are, in effect, finite-difference approximations of the corresponding rarefaction equations. In particular, Eq. (7) is the trapezoidal rule approximation of the integral in Eq. (10), with formal error of $O(\Delta v_S^3)$. Further, we can write

$$|W_S| = \left[-\frac{\Delta p_S}{\Delta v_S} \right]^{1/2},$$

and

$$|V_S| = \frac{[-\Delta p_S/\Delta v_S]}{[1/\Delta v_S] \int_{v_S}^{v_S^*} [-dp/dv]^{1/2}\, dv},$$

and this suggests that

$$|V_S| = |W_S| + O(\Delta v_S^2). \tag{13}$$

This fact is easily verified for the ideal gas case.

This result indiciates that the shock Hugoniot, Eq. (8), is a very good approximation for the corresponding rarefaction equations, Eq. (11), for relatively weak waves. Since rarefaction waves tend to spread out, and so reduce any steep gradients, the specific volume (density) discontinuity between cells in a rarefaction region will generally be small. We therefore expect essentially all rarefaction transitions in Godunov's method to be weak. Thus, we make the replacement

$$|V_S| \simeq |W_S|,$$

that is, we treat rarefaction waves as transitions through rarefaction shocks. This is thus called the two-shock approximation. Although the essentials of this approximation are well known, its first explicit use in a Riemann solver appears to be due to Colella [18].

B. *The Artificial Shock Viscosity Approximation*

We now come to the essential approximation. So far we have established that according to the two-shock approximation we need only work with the shock Hugoniot:

$$\Delta p_S = \mp |W_S|\, \Delta w_S. \tag{8}$$

Let us now consider two examples where an explicit expression for $|W_S|$ exists [12]. For an ideal gas (polytropic) equation of state $p=(\gamma-1)\rho e$, one obtains

$$|W_S| = \tfrac{1}{4}(\gamma+1)\rho_S|\Delta w_S| + \rho_S[a_0^2 + (\tfrac{1}{4}(\gamma+1)\Delta w_S)^2]^{1/2}, \tag{14}$$

where $a_0=(\gamma p_S/\rho_S)^{1/2}$ is the speed of sound ahead of the shock. Similarly, for a simple elastic solid equation of state $p=K(\rho/\rho_0-1)$, we have

$$|W_S| = \tfrac{1}{2}\rho_S|\Delta W_S| + \rho_S[a_0^2 + (\tfrac{1}{2}\Delta w_S)^2]^{1/2}, \tag{15}$$

where $a_0=(K/\rho_0)^{1/2}$ is again the local speed of sound. Notice that these radically different equations of state have remarkably similar shock Hugoniot representations.

Consider the strong and weak shock limits for the pressure jumps:

Strong shock:

$$\Delta p_S = \tfrac{1}{2}(\gamma+1)\rho_S\Delta w_S^2 \qquad \text{for an ideal gas,}$$

$$\Delta p_S = \rho_S\Delta w_S^2 \qquad \text{for an elastic solid,}$$

Weak shock: $\Delta p_S=\rho_S a_0|\Delta w|$, where

$$a_0=(\gamma p_S/\rho_S)^{1/2} \qquad \text{for an ideal gas,}$$

$$a_0=(K/\rho_0)^{1/2} \qquad \text{for an elastic solid.}$$

Observing the similarity of these limiting cases to the expressions for artificial shock viscosity, Eqs. (3) and (4), Wilkins [12] used them to deduce values for the artificial shock viscosity parameters c_0 and c_L.

We now *reverse* this process and use the expression for the combined artificial viscosity, Eq. (5), to approximate the shock Hugoniot. That is, we propose to approximate it by

$$|W_S| = \rho_S(a_S + A_S|\Delta w_S|), \tag{16}$$

where a_S and A_S are material-dependent constants to be determined. We will now proceed to justify this approximation.

Let us start by considering the process of approximating the expressions in Eqs. (14) or (15). These expressions may be written as

$$|W_S| = \rho_S|x|\, G(a_0/|x|),$$

where

$$G(y) = 1 + (1+y^2)^{1/2}, \qquad 0 \leqslant y < \infty, \tag{17}$$

and

$$|x| = \tfrac{1}{4}(\gamma+1)\,|\Delta w_S| \qquad \text{for an ideal gas,}$$

$$|x| = \tfrac{1}{2}|\Delta w_S| \qquad \text{for an elastic solid.}$$

To approximate $G(y)$ we write it as

$$G(y) = 1 + (1 + y)[1 - 2y/(1 + y)^2]^{1/2}$$

and expand the square root term in Taylor's series to obtain a rapidly convergent approximation in the entire range $0 \leqslant y < \infty$:

$$G(y) = 2 + y - \frac{y}{1+y} - \frac{1}{2}\frac{y^2}{(1+y)^3} + \cdots.$$

Truncating to first order we obtain

$$G_1(y) = 2 + y, \tag{18}$$

and therefore

$$|W_S| \simeq \rho_S(a_0 + 2|x|).$$

Thus, the first-order trunctuation corresponds to the approximation incorporated in Eq. (16). Truncating to second order we obtain

$$G_2(y) = 2 + y - \frac{y}{1+y}, \tag{19}$$

and so

$$|W_S| \simeq \rho_S\left[\frac{a_0^2 + 2a_0|x| + 2x^2}{a_0 + |x|}\right].$$

These two approximations are compared in Fig. 2. The second-order approximation is substantially better, but the extra complexity is found to be not

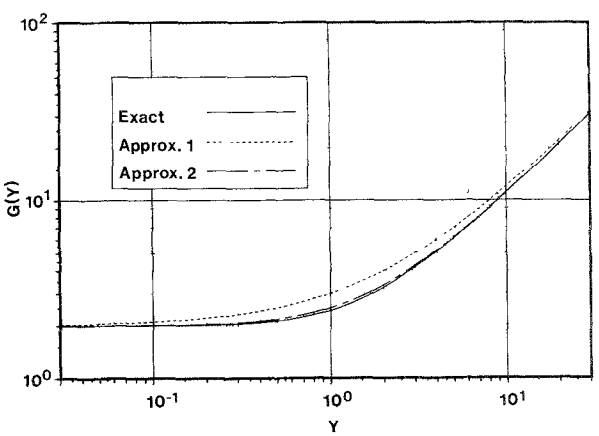

FIG. 2. The comparison of the exact and approximate shock Hugoniots for an ideal gas. The curve labelled Exact represents Eq. (17), Approx. 1 represents Eq. (18), and Approx. 2 represents Eq. (19).

warranted. Further, this method of approximation clearly indicates that the parameter a_S is to be obtained from the weak shock limit,

$$a_S = \lim_{|\Delta w_S|/a_0 \to 0} [|W_S|/\rho_S], \tag{20}$$

and the parameter A_S from the strong shock limit,

$$A_S = \lim_{|\Delta w_S|/a_0 \to \infty} [|W_S|/\rho_S |\Delta w_S|]. \tag{21}$$

We now consider some real materials. Extensive experimental data are available for the shock Hugoniots in numerous solids and liquids [19]. As an example, the data for the Aluminum alloy 6061 presented in Fig. 3 are typical. Unless the material exhibits a phase transition the data are usually well fitted by a straight line,

$$U_S = a_S + A_S U_p, \tag{22}$$

where U_S is the shock speed into material at rest, and U_p is the corresponding particle velocity behind the shock. For Aluminum 6061 these coefficients are $a_S =$ 5.35 km/s and $A_S = 1.34$. Using the Rankine–Hugoniot relations, it can be shown that Eq. (22) exactly corresponds to our assumed shock Hugoniot:

$$\Delta p_S = \rho_S(a_S + A_S|\Delta w_S|)\,\Delta w_S. \tag{16}$$

Thus, to the extent that Eq. (22) fits the available data there is *no approximation* in using Eq. (16) for the shock Hugoniot in such materials.

In the general case we may use Eqs. (20) and (21) and the Rankine–Hugoniot relations to deduce that

$$a_S = \left[\left.\frac{\partial p}{\partial \rho}\right|_S + \frac{p_S}{\rho_S^2}\left.\frac{\partial p}{\partial e}\right|_S\right]^{1/2}, \tag{23}$$

$= a_0$, the local equation of state speed of sound,

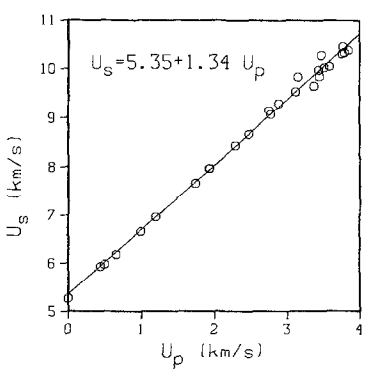

FIG. 3. Experimental shock Hugoniot data for Aluminum 6061. Reproduced, by permission of the publisher, from Ref. 19.

and

$$A_S = \lim_{|\Delta w_S|/a_0 \to \infty} \left[\frac{\rho_S^*/\rho_S}{\rho_S^*/\rho_S - 1} \right]. \tag{24}$$

That is, the parameter A_S is given in terms of the density ratio in the limit of very strong shocks. Hence, this parameter is also deduced from the equation of state and the Rankine–Hugoniot relations.

C. *The Solution of the Approximate Riemann Problem*

We have established the general form of the approximate shock Hugoniot, Eq. (16), and therefore also of the rarefaction Hugoniot, by the two-shock approximation. This allows us to formulate the Riemann problem equations. First consider rightward-propagating waves. For a shock, we have

$$p^* - p_R = \rho_R (a_R + A_R \Delta w_R) \Delta w_R, \tag{25}$$

where we have removed the absolute value sign because $\Delta w_R > 0$ in this case. This is also the equation for a rightward rarefaction wave because of the second degree contact (C^2 continuity) implied by Eq. (13). However, a physically realistic rightward Hugoniot curve must have positive slope, and so this equation is only valid for

$$w^* \geqslant w^*_{\min} \equiv w_R - a_R/2A_R.$$

For numerical purposes, we continue this Hugoniot curve to all values of w^* as follows:

$$p^* - p_R^* = \rho_R A_R |w^* - w^*_{\min}| (w^* - w_{\min}), \tag{26}$$

where $p_R^* \equiv p_R - \frac{1}{4} \rho_R a_R^2 / A_R$.

Similarly, for leftward-going shocks, we have

$$p^* - p_L = -\rho_L (a_L - A_L \Delta w_L) \Delta w_L, \tag{27}$$

where we have again removed the absolute value sign by allowing for the proper sign of Δw_L. By continuation, this is also the equation for a leftward rarefaction wave, except that to maintain the physically correct negative slope in this region, we must restrict it to

$$w^* \leqslant w^*_{\max} \equiv w_L + a_L/2A_L.$$

Again, for numerical purposes we regularize Eq. (27) as follows:

$$p^* - p_L^* = -\rho_L A_L |w^* - w^*_{\max}| (w^* - w^*_{\max}), \tag{28}$$

where $p_L^* \equiv p_L - \frac{1}{4} \rho_L a_L^2 / A_L$.

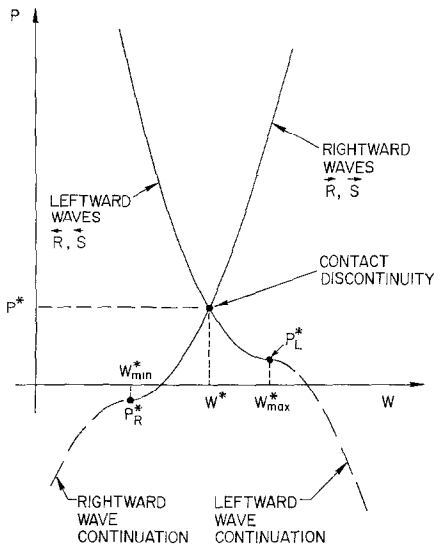

FIG. 4. An illustration of a graphical method of solution of the approximate Riemann problem in the p–w plane.

Equations (26) and (28) specify the approximate Riemann problem. The graphical solution of these two equations is illustrated in Fig. 4. Clearly, there is a unique solution (p^*, w^*) at the intersection of the two monotone curves of opposite slope. The solution is found explicitly by eliminating p^* between Eqs. (26) and (28) to obtain

$$\rho_R A_R |w^* - w^*_{min}| (w^* - w^*_{min}) + \rho_L A_L |w^* - w^*_{max}| (w^* - w^*_{max}) + p^*_R - p^*_L = 0.$$

This a semi-quadratic equation for w^*. It can be converted into a quadratic equation by assuming a sign for $(w^* - w^*_{min})$ and $(w^* - w^*_{max})$. There are four cases to be considered. One of the two roots of each quadratic equation can be eliminated a priori. The unique solution is that root, out of the remaining four possibilities, which is consistent with the initial assumption regarding the sign of $(w^* - w^*_{min})$ and $(w^* - w^*_{max})$. A FORTRAN subroutine for the solution is given in the Appendix. The calculation is arranged so that the most probable case $(w^*_{min} < w^* < w^*_{max})$ is calculated first, such that on the average little more than one case will be calculated. Thus, this algorithm is best suited to serial computers, but a vectorizable version is easily obtained at the expense of computing all four cases. Having calculated the interface velocity w^*, the pressure is most conveniently obtained by combining Eqs. (26) and (28):

$$p^* = \tfrac{1}{2}(p^*_L + p^*_R) + \tfrac{1}{2}\rho_R A_R |w^* - w^*_{min}| (w^* - w^*_{min}) - \tfrac{1}{2}\rho_L A_L |w^* - w^*_{max}| (w^* - w^*_{max}).$$

If desired, the density and internal energy on either side of the interface may be obtained by using Eqs. (6) and (7).

If an interface is such that it cannot support tension, then the Riemann problem can predict cavitation. In such a case, if p^* is found to be negative, then we set $p^* = 0$ and calculate two interface velocities by solving Eqs. (26) and (28). This is an interesting bit of physics which is inherent in the Godunov method, but which is ruled out in other methods, including the method of artificial shock viscosity.

IV. Numerical Comparisons

Let us begin by considering the quintessential problem for any shock capturing scheme: the resolution of a shock profile. Figures 5 and 6 illustrate the Lagrangian Godunov calculations of a steady, infinite strength shock propagating in an ideal gas with $\gamma = \frac{5}{3}$. The shock profile is nearly optimally resolved over two or three cells, with no oscillations. Figure 5 is the calculation with the approximate Riemann solver, while Fig. 6 is the same calculation with the exact Riemann solver. The difference between the two solutions is barely detectable. However, this problem tests only compressive flows, and the test is not very stringent since the approximation is, in a sense, biased towards the shock Hugoniot.

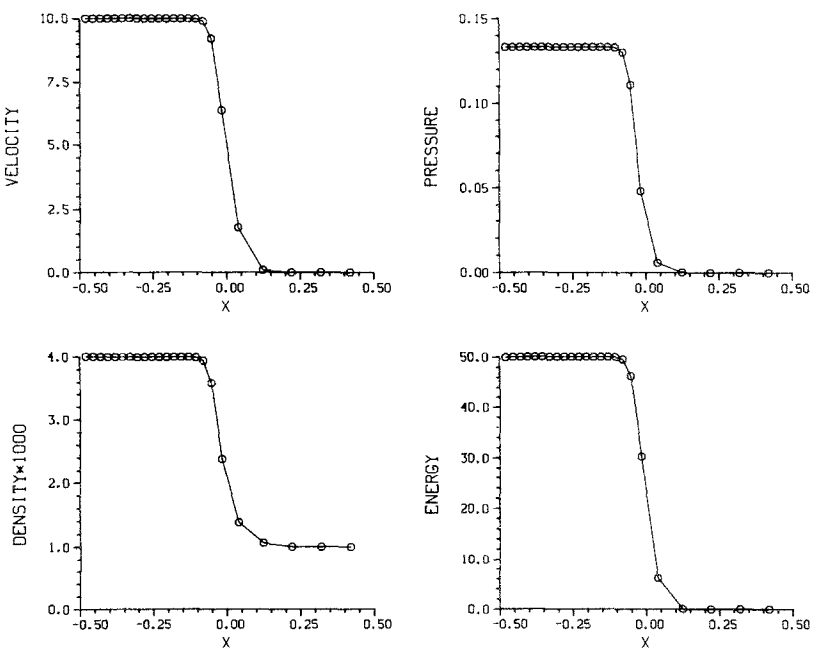

FIG. 5. A Lagrangian Godunov's method solution of the steady, 1-dimensional propagation of an infinite strength shock in a $\gamma = \frac{5}{3}$ gas using the approximate Riemann solver.

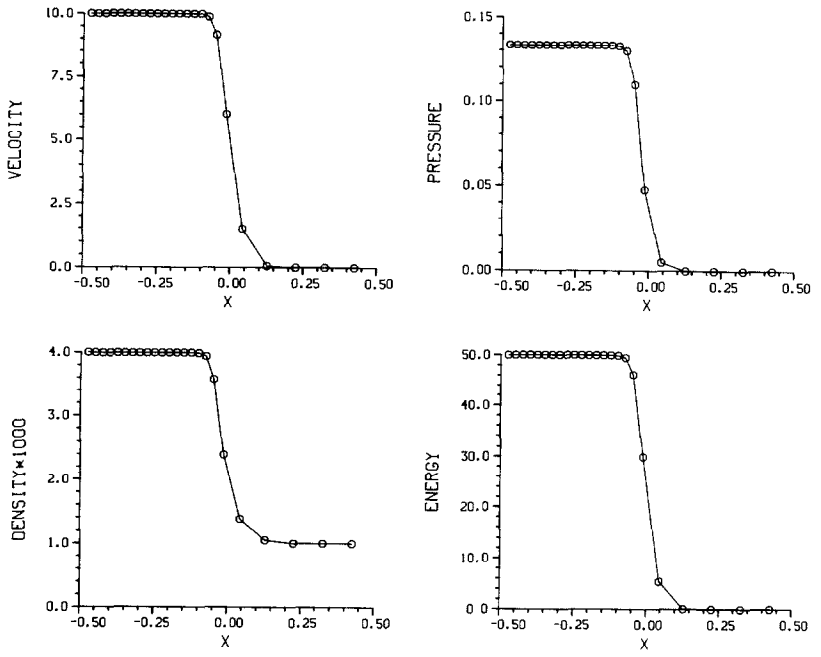

FIG. 6. The same problem and solution method as in Fig. 5, except that an exact Riemann solver was used.

The accuracy of the approximation for the solution of an actual shock tube Riemann problem ($w_L = w_R = 0$) is illustrated in Table I, for a range of diaphragm pressure ratios, and for $\gamma = \frac{7}{5}$ and $\gamma = \frac{5}{3}$. The values of the contact discontinuity pressure p^* and velocity w^* calculated by the approximate Riemann solver are surprisingly good in spite of the presence of a strong rarefaction wave in all cases considered. Recall that the approximation has been developed for use in a Godunov method where essentially all rarefaction waves are expected to be weak.

Another stringent test problem is the Godunov method calculation of the shock tube problem specified by Sod [20]. For this problem we have $\rho_L = p_L = 1$, $\rho_R = \frac{1}{8}$, $p_R = \frac{1}{10}$, $\gamma = \frac{7}{5}$, $\Delta x = 0.01$, and the total length $L = 1$. Figure 7 shows the calculation with the approximate Riemann solver, and Fig. 8 with the exact Riemann solver. The main difference between these two calculations is to be observed at the contact discontinuity where the typical Lagrangian "starting process" for an impulsively started piston is affected by the inaccuracy of the approximate Riemann problem for a strong rarefaction wave, discussed in the previous paragraph. However, once the rarefaction fan evolves and spreads out over several cells it becomes difficult to distinguish a difference between results of the approximate and exact Riemann solver calculations in the rarefaction region, as well as in the shock region.

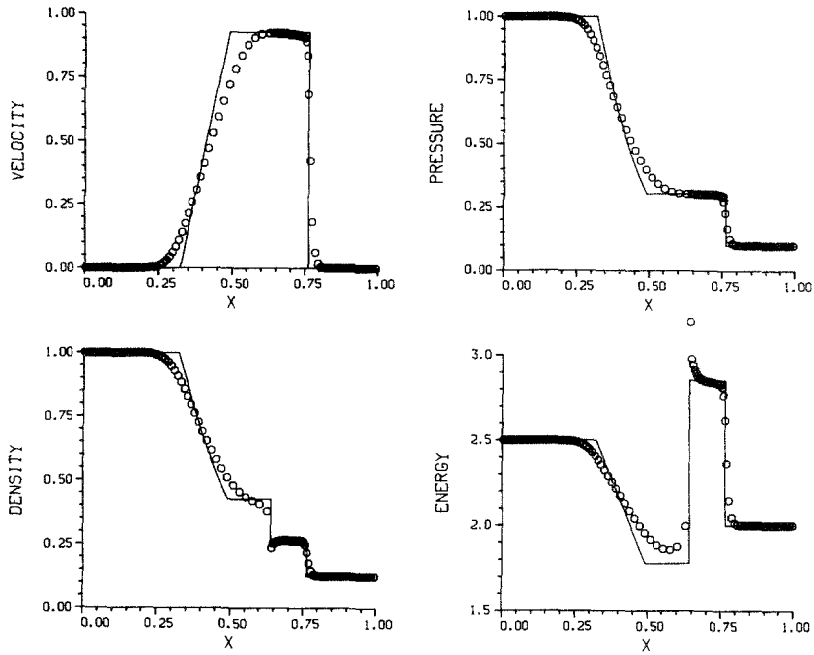

FIG. 7. Sod's shock tube problem solution using a Lagrangian Godunov's method and the approximate Riemann solver.

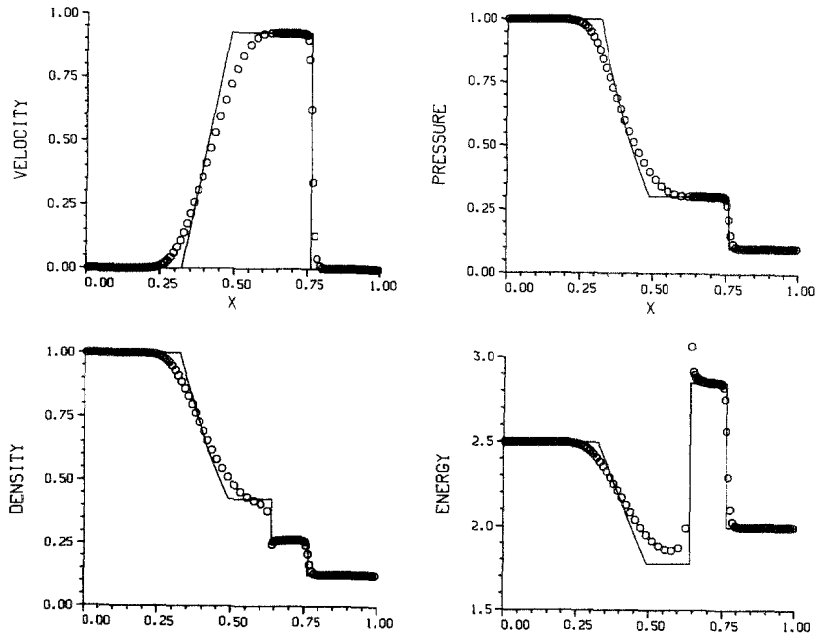

FIG. 8. The same problem and solution method as in Fig. 7, except that an exact Riemann solver was used.

TABLE I

Comparison of the Exact and Approximate Riemann Solver for a Shock Tube Problem ($p_R = e_R = e_L = 1$, $w_L = w_R = 0$)

	Exact		Approximate	
p_L	p^*	w^*	p^*	w^*
Case (a) $\gamma = \frac{7}{5}$				
2	1.40	0.29	1.49	0.32
4	1.93	0.59	2.54	0.74
6	2.30	0.76	3.04	0.90
8	2.60	0.88	3.33	0.97
10	2.85	0.97	3.52	1.04
12	3.06	1.05	3.65	1.07
14	3.26	1.11	3.75	1.10
16	3.43	1.17	3.82	1.12
18	3.58	1.22	3.88	1.13
20	3.73	1.26	3.93	1.15
22	3.86	1.30	3.97	1.16
24	3.99	1.34	4.01	1.16
Case (b) $\gamma = \frac{5}{3}$				
2	1.40	0.27	1.48	0.29
4	1.91	0.53	2.52	0.69
6	2.26	0.69	3.06	0.85
8	2.53	0.80	3.36	0.93
10	2.76	0.88	3.56	0.98
12	2.96	0.95	3.69	1.02
14	3.13	1.00	3.80	1.04
16	3.28	1.05	3.88	1.06
18	3.42	1.09	3.94	1.08
20	3.55	1.13	3.99	1.09
22	3.67	1.17	4.03	1.10
24	3.77	1.20	4.07	1.11

V. Discussion

We have stressed the close connection between the artificial shock viscosity method and Godunov's method in the sense that both methods supply an appropriate amount of entropy in order to "capture" shocks in a discrete mesh. This connection has suggested a simple quadratic form for an approximate shock Hugoniot, with only two material-dependent parameters. The resulting approximate Riemann solver retains the essentials quadratic nonlinearity which enables it to deal with the entire range of conditions from weak sound waves to strong shocks.

It is important to appreciate that the resulting method is not just a variation of

the artificial viscosity method, but a very general simplification of Godunov's method, which retains all of its essential properties. Some of the more important properties may be summarized as follows:

(a) All variables are cell-centered. Only the normal component of velocity is defined at cell interfaces by the Riemann problem. This is the natural way to define the motion of cell boundaries in a Lagrangian calculation, and it facilitates the treatment of material interfaces where slip (tangential velocity discontinuity) may occur.

(b) The use of a Riemann problem makes Godunov's method a form of the method of characteristics. The proper domain of influence of the hyperbolic system of equations being solved is accounted for.

(c) Shocks are "captured" with nearly optimal resolution on a given mesh, with no mesh dependent parameters.

(d) Physical effects such as cavitation can be predicted.

The importance of the use of this new Riemann solver in Godunov's method is that it combines the computational economy of the artificial shock viscosity method with the above important characteristics of Godunov's method. Unlike some previous approximate Riemann solvers it is applicable to materials with arbitrary equations of state.

The close agreement of calculations with the exact and approximate Riemann solvers when used in Godunov's method suggests that the degree of approximation of the Riemann problem is more than adequate. Indeed, as Roe points out [7] an accurate solution is worthwhile only if the information so obtained is put to some sophisticated use. The more accurate approximation to the shock Hugoniot in an ideal gas, Eq. (19), if used would require the solution of quartic equations, and this is clearly not warranted. Finally, the material-dependent parameters a_S and A_S are sufficiently well defined by Eqs. (23) and (24), or by Eq. (22), that they are readily obtainable for most materials of interest. However, even if their value is uncertain the sensitivity of calculations to their variation appears to be low. This may be due to the possibility, suggested by the analogy with artificial shock viscosity, that the effects are largely accounted for by changing the amount of dissipation introduced into the calculation.

ACKNOWLEDGMENTS

I thank J. R. Baumgardner, D. E. Carroll, B. A. Kashiwa, and H. M. Ruppel for putting this method to practical use and for persevering through the early stages of its development. This work was supported by the U.S. Department of Energy.

APPENDIX:
COMPUTER PROGRAM FOR THE APPROXIMATE RIEMANN PROBLEM SOLVER

```
      SUBROUTINE RIEMANN
      COMMON /RIEMIN/ WL,WR,RHOL,RHOR,PL,PR,SSL,SSR,AL,AR
      COMMON /RIEMOUT/ P12,W12
C ***
C *** APPROXIMATE RIEMANN PROBLEM SOLVER
C *** TWO SHOCK APPROXIMATION
C *** ARTIFICIAL SHOCK VISCOSITY APPROXIMATION
C *** JOHN K. DUKOWICZ   T-3   MAY 1984
C ***
C *** INPUT: WL,WR -- VELOCITIES TO THE LEFT AND RIGHT OF THE INTERFACE,
C ***                 NORMAL TO THE INTERFACE, POSITIVE TO THE RIGHT
C ***        RHOL,RHOR -- DENSITIES
C ***        PL,PR -- PRESSURES
C ***        SSL,SSR -- SOUND SPEEDS
C ***        AL,AR -- STRONG SHOCK DENSITY RATIO PARAMETERS
C *** OUTPUT: P12 -- INTERFACE PRESSURE
C ***         W12 -- INTERFACE VELOCITY
C ***
      WMIN=WR-0.5*SSR/AR
      WMAX=WL+0.5*SSL/AL
      PLMIN=PL-0.25*RHOL*SSL**2/AL
      PRMIN=PR-0.25*RHOR*SSR**2/AR
      BL=RHOL*AL
      BR=RHOR*AR
      A=(BR-BL)*(PRMIN-PLMIN)
      B=BR*WMIN**2-BL*WMAX**2
      C=BR*WMIN-BL*WMAX
      D=BR*BL*(WMIN-WMAX)**2
C ***
C *** CASE A:  W12-WMIN>0, W12-WMAX<0
C ***
      DD=SQRT(AMAX1(0.,D-A))
      W12=(B+PRMIN-PLMIN)/(C-SIGN(DD,WMAX-WMIN))
      IF (W12-WMIN.GE.0..AND.W12-WMAX.LE.0.) GO TO 10
C ***
C *** CASE B:  W12-WMIN<0, W12-WMAX>0
C ***
      DD=SQRT(AMAX1(0.,D+A))
      W12=(B-PRMIN+PLMIN)/(C-SIGN(DD,WMAX-WMIN))
      IF (W12-WMIN.LE.0..AND.W12-WMAX.GE.0.) GO TO 10
      A=(BL+BR)*(PLMIN-PRMIN)
      B=BL*WMAX+BR*WMIN
      C=1./(BL+BR)
C ***
C *** CASE C:  W12-WMIN>0, W12-WMAX>0
C ***
      DD=SQRT(AMAX1(0.,A-D))
      W12=(B+DD)*C
      IF (W12-WMIN.GE.0..AND.W12-WMAX.GE.0.) GO TO 10
C ***
C *** CASE D:  W12-WMIN<0, W12-WMAX<0
C ***
      DD=SQRT(AMAX1(0.,-A-D))
      W12=(B-DD)*C
   10 P12=0.5*(PLMIN+PRMIN+BR*ABS(W12-WMIN)*(W12-WMIN)-BL*ABS(W12-WMAX)
     1 *(W12-WMAX))
      RETURN
      END
```

REFERENCES

1. J. VON NEUMANN AND R. D. RICHTMYER, *J. Appl. Phys.* **21** (1950), 232.
2. S. K. GODUNOV, *Mat. Sb.* **47** (1959), 271.
3. R. D. RICHTMYER AND K. W. MORTON, "Difference Methods for Initial Value Problems," 2nd ed., Interscience, New York, 1967.
4. P. L. ROE, *in* "Proceedings, Seventh International Conference on Numerical Methods in Fluid Dynamics," Springer-Verlag, New York/Berlin, 1981.
5. S. K. GODUNOV, A. V. ZABRODIN, AND G. P. PROKOPOV, *USSR Comput. Math. Math. Phys. (Engl. Transl.)* **1** (1961), 1187.
6. B. ENQUIST AND S. OSHER, *Math. Comput.* **34** (1980), 45.
7. P. L. ROE, *J. Comput. Phys.* **43** (1981), 357.
8. M. PANDOLFI, *AIAA J.* **22** (1984), 602.
9. B. VAN LEER, *J. Comput. Phys.* **32** (1979), 101.
10. P. COLLELA AND P. R. WOODWARD, *J. Comput. Phys.* **54** (1984), 174.
11. P. R. WOODWARD AND P. COLELLA, *J. Comput. Phys.* **54** (1984), 115.
12. M. L. WILKINS, *J. Comput. Phys.* **36** (1980), 281.
13. J. K. DUKOWICZ, *J. Comput. Phys.* **54** (1984), 411.
14. P. A. THOMPSON, "Compressible-Fluid Dynamics," McGraw–Hill, New York, 1972.
15. R. LANDSHOFF, "A Numerical Method for Treating Fluid Flow in the Presence of Shocks," Los Alamos Scientific Laboratory Report LA-1930, Los Alamos, N.M., 1955.
16. R. COURANT AND K. O. FRIEDRICHS, "Supersonic Flow and Shock Waves," Interscience, New York, 1948.
17. P. COLELLA AND H. M. GLAZ, "Efficient Solution Algorithms for the Riemann Problem for Real Gases," Lawrence Berkeley Laboratory Report LBL-15776, Berkeley, Calif., 1983.
18. P. COLELLA, *SIAM J. Sci. Statist. Comput.* **3** (1982), 76.
19. S. P. MARSH, "LASL Shock Hugoniot Data," Univ. of California Press, Berkeley/Los Angeles, 1980.
20. G. A. SOD, *J. Comput. Phys.* **27** (1978), 1.